Original Article

Bioinformatic prediction of miR-320a as a potential negative regulator of CDGSH iron-sulfur domain 2 (*CISD2*), involved in lung adenocarcinoma bone metastasis via MYC activation, and associated with tumor immune infiltration

Xiaoxi Zhao[1], Lei Li[2], Yancheng Li[2], Yanxiao Liu[2], Hua Wang[2], Nika Samadzadeh Tabrizi[3], Zhou Ye[2], Ziru Zhao[2]

[1]Department of Ultrasound Medicine, Quzhou People's Hospital, Quzhou, China; [2]Department of Spinal Surgery, Quzhou People's Hospital, Quzhou, China; [3]Department of Thoracic Surgery, Albany Medical Center, Albany, NY, USA

Contributions: (I) Conception and design: X Zhao, Z Zhao; (II) Administrative support: None; (III) Provision of study materials or patients: L Li, Y Li; (IV) Collection and assembly of data: Y Liu, Z Ye; (V) Data analysis and interpretation: H Wang; (VI) Manuscript writing: All authors; (VII) Final approval of manuscript: All authors.

Correspondence to: Ziru Zhao, PhD; Zhou Ye, PhD. Department of Spinal Surgery, Quzhou People's Hospital, No. 100 Minjiang Avenue, Kecheng District, Quzhou 324000, China. Email: Zhaoziru0809@163.com; yezhou133@126.com.

Background: Ferroptosis, a form of regulated cell death associated with iron-dependent lipid peroxidation, plays a role in cancer progression. However, the specific mechanisms of ferroptosis in lung adenocarcinoma (LUAD) bone metastasis (BM) remain unclear. Using bioinformatics analysis, this study sought to identify the ferroptosis-associated genes involved in BM in LUAD, thus providing potential novel targets for the treatment of BM in LUAD.

Methods: The RNA expression dataset GSE10799 was acquired from the Gene Expression Omnibus (GEO) database, and intersected with the ferroptosis dataset to identify ferroptosis-related differentially expressed genes (DEGs). The expression of candidate genes and their correlation with the prognosis of LUAD patients were validated in The Cancer Genome Atlas (TCGA) database. A protein gene interaction network was constructed using GeneMania and Retrieval of Interacting Genes/Proteins (STRING) databases. The association between the candidate genes and immune cells was assessed via TCGA and Tumor IMmune Estimation Resource (TIMER) databases. The potential mechanisms were elucidated by a gene set enrichment analysis (GSEA). The relevant microRNAs (miRNAs or miRs) that bind to the 3'untranslated region (3'UTR) end of candidate genes' mRNA was explored using the TargetScan database. The expression of these candidate miRNAs in LUAD was validated and the correlation between candidate miRNAs and candidate mRNAs was tested using the TCGA database. Finally, the clinical data of 40 LUAD patients were retrospectively analyzed to evaluate the clinical value of candidate gene expression for LUAD BM patients.

Results: In this research, 15 ferroptosis-related DEGs in LUAD BM were identified. TCGA database analysis indicated that patients with low levels of CDGSH iron-sulfur domain 2 (*CISD2*) in LUAD had better disease-specific survival (DSS), overall survival (OS), and a better progression-free interval (PFI) than those with high levels of *CISD2*. The TIMER database results show that the expression of *CISD2* is correlated with the infiltration levels of various immune cells. The GSEA indicated that *CISD2* might influence biological activity in LUAD by participating in cell-cycle regulation, mitochondrial translation, DNA damage repair, c-*Myc* (*MYC*) activation, and the P53 signaling pathway. Through the combined analysis of the TargetScan and TCGA databases, hsa-miR-320a was identified as the optimal upstream regulatory miRNA. The immunohistochemistry data indicated that the positive CISD2 expression rates and immunohistochemistry scores of the patients with BM were significantly higher than those of the patients without BM ($P<0.05$). The high expression of CISD2 is a significant risk factor for BM in LUAD.

Conclusions: The downregulation of *CISD2* expression may extend DSS, OS, and the PFI of LUAD

patients. Thus, *CISD2* could serve as a novel predictive biomarker for LUAD patients. Further, miR-320a might negatively regulate *CISD2* and participate in LUAD BM by activating *MYC*. These data provide a potential perspective for developing anticancer therapies for LUAD-BM patients.

Keywords: Lung adenocarcinoma (LUAD); bone metastasis (BM); ferroptosis; bioinformatics analysis; prognosis

Submitted Jul 11, 2024. Accepted for publication Aug 20, 2024. Published online Aug 27, 2024.
doi: 10.21037/tcr-24-1188
View this article at: https://dx.doi.org/10.21037/tcr-24-1188

Introduction

According to the International Agency for Research on Cancer in 2022, lung cancer (LC) is the most commonly diagnosed cancer worldwide (with an incidence of 12.4%), and a leading cause of cancer-related deaths (with a mortality rate of 18.7%) (1). The 5-year overall survival (OS) rates for LC range from 14% to 17% (2) with metastasis serving as the primary cause of death (3). The most common type of LC is lung adenocarcinoma (LUAD), which accounts for approximately 55% of cases (4). The 5-year OS rate of patients with late-stage disease is less than 15% (4).

Skeletal involvement is a common occurrence in LUAD metastasis and often presents as osteolytic bone metastasis (BM) (5,6). BM in LC typically presents with bone pain, nerve compression, and hypercalcemia, and significantly affects the quality of life of patients (7). The heterogeneity of tumor cells and the development of resistance to conventional therapies complicate treatment efforts, emphasizing the need for personalized comprehensive treatments tailored to individual patients.

The identification of molecular indices and differential genes for diagnosis could help to assess the biomolecular mechanisms related to LUAD BM, thus advancing the efficacy of gene-targeted therapies. Currently, various studies involving tumor markers (e.g., proteins, peptides, metabolites, and nucleic acids) are underway. Variations in tumor markers can correspond to different stages of cancer development (8), providing a valuable complement to imaging techniques. However, while these markers show promise, their limited specificity and sensitivity in certain contexts highlight the need for further research and development.

One approach to gene-targeted therapy involves inducing programmed cell death in cancer cells. Ferroptosis is a type of programmed cell death that is characterized by the production and accumulation of iron-dependent lipid peroxidation (9,10). A growing body of literature has shown the potential role of ferroptosis in BM (11). For example, semiconductor polymer nanoinductors have been used to induce ferroptosis and amplify oxidative damage, offering a synergistic approach for treating BM (11). In 2023, Zhou *et al.* (12) used bioinformatics to identify ferroptosis-related differentially expressed genes (DEGs) in LUAD BM, providing new targets for monitoring and treating BM. Additionally, whether used individually or in combination, the serum markers alkaline phosphatase (ALP) and neuron-specific enolase (NSE) both demonstrated an area under the

Highlight box

Key findings

- CDGSH iron-sulfur domain 2 (*CISD2*) is a novel gene in patients with lung adenocarcinoma (LUAD) who suffer from metastatic disease to the bone.
- The reduced expression of *CISD2* is associated with a better patient prognosis; thus, *CISD2* may serve as a novel predictive biomarker in patients with LUAD with metastatic bone disease.

What is known, and what is new?

- Ferroptosis, a form of regulated cell death associated with iron-dependent lipid peroxidation, plays a role in cancer progression. The involvement of ferroptosis-related genes in cancer metastasis, particularly in LUAD, has been increasingly recognized.
- This study identifies *CISD2* as a key ferroptosis-related gene in LUAD bone metastasis (BM). The research demonstrates that high *CISD2* expression is a significant risk factor for BM in LUAD and suggests that miR-320a may regulate *CISD2*, influencing LUAD progression and providing a new target for potential therapies.

What is the implication, and what should change now?

- This study lays the groundwork for future clinical studies to examine the role of *CISD2* and its related indicators to help clinicians better predict the prognosis of LUAD patients with BM. Research on microRNA-320a and its regulatory network will provide direction for the development of novel therapeutic strategies to optimize the management and outcomes of patients with LUAD with metastatic bone disease.

curve >0.70.

However, the specific mechanisms of ferroptosis in LUAD BM remain unclear. This study evaluated the DEGs in LUAD-BM tissues compared to normal lung tissues. The identified DEGs were subsequently intersected with the ferroptosis dataset to acquire the ferroptosis-associated DEGs. Further, to determine essential bio-indices and establish the pathogenesis of LUAD BM at the molecular level, upstream regulatory microRNAs (miRNAs or miRs) were investigated. Finally, we integrated clinical data from Quzhou People's Hospital LC patients to explore clinical factors for evaluating LUAD BM. In doing so, we sought to further delineate the role of ferroptosis in LUAD-BM patients. We present this article in accordance with the STREGA reporting checklist (available at https://tcr.amegroups.com/article/view/10.21037/tcr-24-1188/rc).

Methods

Identifying the DEGs in LUAD BM

The gene expression dataset, GSE10799, which comprises both normal and LUAD-BM tumor tissues, was acquired from the Gene Expression Omnibus (GEO) (https://www.ncbi.nlm.nih.gov/geo/query/acc.cgi) database using GEOquery. Additional probes corresponding to multiple molecules were removed. When encountering probes for the same molecule, only those with the highest signal were retained.

For the differential expression analysis, an e-tool, Gene Expression Omnibus 2 R (GEO2R; https://www.ncbi.nlm.nih.gov/geo/geo2r/) was used. Genes that were differentially expressed in LUAD BM were retained if they met the following criteria: |log2 (fold change)|>0.5, with an adjusted P value <0.05.

Ferroptosis-related genes

Ferroptosis-related genes were acquired from the ferroptosis database (http://www.zhounan.org/ferrdb). The dataset comprises 259 genes, including 108 driver genes and 69 suppressor genes, and 111 genetic markers (13).

Identifying ferroptosis-related DEGs in LUAD BM

The genes acquired from the ferroptosis database were cross-referenced with GSE10799 to identify the potential ferroptosis-related DEGs, which are hereafter referred to as the candidate genes. Venn diagrams and heat maps were prepared using Venny 2.1 and Heml software (http://www.liuxiaoyuyuan.cn/), respectively.

Identifying candidate gene-gene interactions

Using GeneMANIA database (http://www.genemania.org) and the STRING database (https://string-db.org/), the key genes were first entered as the query. Both databases offer a wide range of options for analyzing and predicting gene interactions, including protein-protein interactions (PPIs), protein-DNA interactions, genetic interactions, common pathway involvement, physiological and biochemical reactions, similarity in gene and protein expression patterns, shared protein domains, and phenotype associations. Taking into account these different types of interactions and sources of evidence, a comprehensive network of interactions was constructed. After constructing a PPI network, we focused on the key nodes and edges within the network, especially those nodes that have significant interactions with multiple genes or proteins, as they may play a central role in biological processes. Then, we further analyzed the network's topology, including the degree distribution of nodes, clustering coefficients, and path lengths, to reveal the overall organizational principles and potential functional modules of the network. Through network analysis, a group of genes and proteins closely related to key genes can be identified, which may play a synergistic role in common biological pathways or processes. This information provides important clues for further understanding the functions and regulatory mechanisms of key genes.

Relationships between candidate genes and immune cells

Using the Tumor IMmune Estimation Resource (TIMER) (https://cistrome.shinyapps.io/timer/) and The Cancer Genome Atlas (TCGA) databases, the expression of the candidate ferroptosis-related DEGs in LUAD was assessed and portrayed using bar graphs. Kaplan-Meier survival curves were generated from the Gene Expression Profiling Interactive Analysis (GEPIA) website (http://gepia.cancer-pku.cn/).

Gene set enrichment analysis (GSEA)

The online functional analysis was carried out using the DEGs via the Metascape database (https://metascape.org/gp/index.html#/main/step1).

Prediction of the upstream regulated MiRNAs of the candidate genes

To determine whether the candidate genes were modulated by upstream genes, the miRNAs that interact with the 3'untranslated region (3'UTR) end of the messenger RNA (mRNA) were identified from the TargetScan database (https://www.targetscan.org/vert_80/).

Testing the association between the candidate miRNAs and essential genes in TCGA

To evaluate whether the select candidate genes were regulated by upstream genes, we further explored the possible miRNAs associated with the 3'UTR end binding of the mRNA of the select candidate genes through the TargetScan database.

Inclusion of LUAD patients' clinical data

A retrospective analysis of 40 LUAD patients admitted to the Quzhou People's Hospital from May 2021 to May 2023 was performed. To be eligible for inclusion in this study, the patients had to meet the following inclusion criteria: (I) have pathologically confirmed LUAD; (II) have complete clinical data; and (III) have complied and cooperated with the relevant tests. Patients were excluded from the study if they met any of the following exclusion criteria: (I) had received glucocorticoid or bisphosphonate treatment within 3 months of enrollment; (II) had another severe lung disease, including asthma; and/or (III) had another concurrent cancer. The study was conducted in accordance with the Declaration of Helsinki (as revised in 2013). The study was approved by the Ethics Committee of Quzhou People's Hospital (No. 2023-015) and informed consent was taken from all the patients.

Tissue microarray construction and immunohistochemistry

Specimens of surgically resected LUAD and adjacent tissue (5 cm from the cancer tissue) were collected, paraffin-embedded, sliced (4-μm thick), dewaxed in xylene, rehydrated using gradient ethanol concentration, subjected to an antigen retrieval process by heating in citrate buffer for 20 minutes, treated with hydrogen peroxide (3%) for 10 minutes at ambient temperature to block the activity of endogenous peroxidase, and then blocked using 10% fetal bovine serum for 10 minutes at ambient temperature. The samples were then treated overnight with CISD2 antibody (PA5-53398, Thermo Fisher Scientific, Waltham, MA, USA) at 4 ℃, followed by horseradish peroxidase-conjugated goat anti-rabbit immunoglobulin G secondary antibody (Zhongshan Golden Bridge Biotechnology Co., Ltd., Beijing, China) at ambient temperature for 20 minutes, stained with 3,3'-diaminobenzidine, and coverslipped with neutral resin. The scores were based on the percentages of positively stained cells as follows: 4 (>75%), 3 (51–75%), 2 (25–50%), 1 (<25%), and 0 (negative). The staining intensity was scored as follows: 3 (strong positive), 2 (moderate positive), 1 (weak positive), and 0 (negative or no staining). For each specimen, the final score represented the product of the two scores. After assessing the average of these scores, samples with a score <4 were defined as having a negative expression of the select candidate gene CISD2.

Statistical analysis

R (version 3.6.3; R Foundation for Statistical Computing, Vienna, Austria) was employed for the statistical assessment and visualization. The possible cellular mechanisms of the crucial gene *CISD2* were assessed via a GSEA. To assess the patient survival rate, the Kaplan-Meier test was employed, while the log-rank statistical test was used for significance testing. Statistical analyses in the rest of the studies were automatically calculated by the specific online databases. The statistically significant threshold was set as a log-rank P value <0.05 or a P value <0.05.

Results

Screening of the DEGs

We acquired the microarray expression dataset GSE10799 from the GEO database. By comparing the tumor tissue to the normal tissue, volcano and principal component analysis plots of the DEGs were constructed (*Figure 1A*,*1B*, respectively). Subsequently, these DEGs were intersected with the ferroptosis-associated genes to obtain a Venn diagram of the two data sets (*Figure 1C*). Ultimately, the following 15 ferroptosis-related DEGs in LUAD BM were identified: *TP63*, *DPP4*, *LURAP1L*, *EGFR*, *HSD17B11*, *ISCU*, *CISD2*, *CHMP5*, *PEBP1*, *IDH1*, *TNFAIP3*, *LONP1*, *ELAVL1*, *MT3*, and *SLC2A8*.

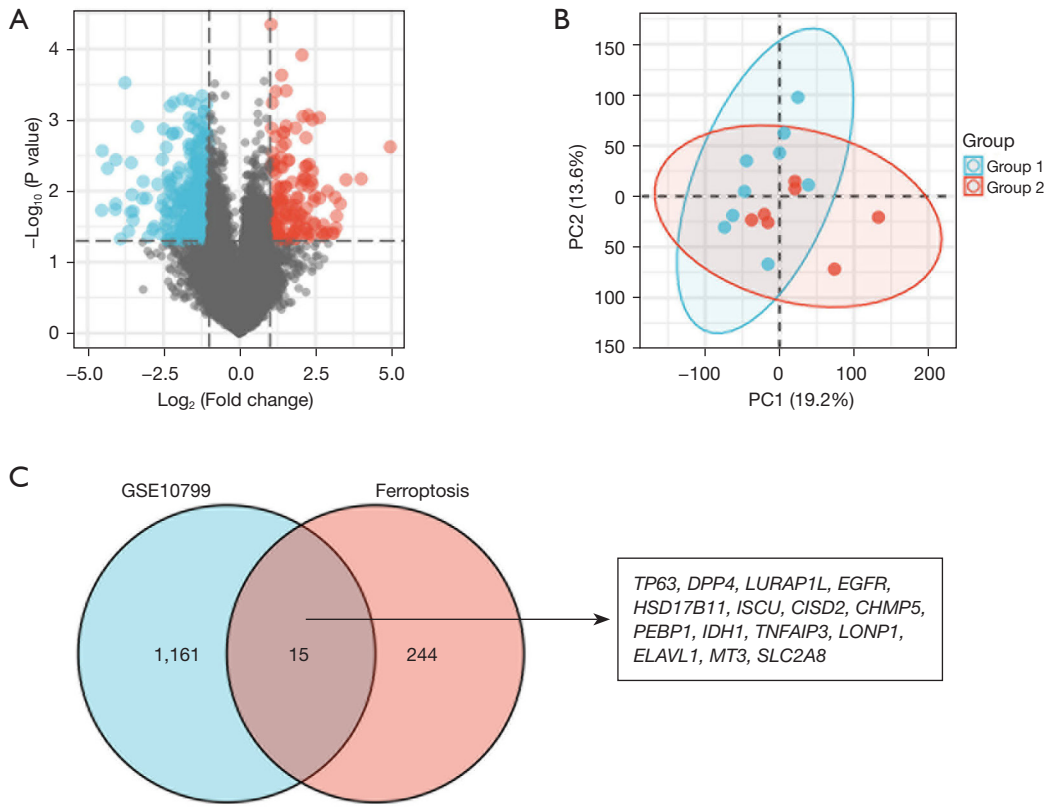

Figure 1 Identification of DEGs. (A) Volcano plot and (B) PCA plot of the DEGs in GSE10799 (blue represents low expression DEGs, red represents high expression DEGs, and gray section represents genes that are not significantly and differentially expressed); (C) Venn diagram showing the intersection between ferroptosis-associated genes and DEGs in lung cancer BM. PCA, principal component analysis; DEGs, differentially expressed genes; BM, bone metastasis.

Expression of the candidate genes in LUAD

The LUAD-TCGA dataset was used to identify the expression of the aforementioned 15 candidate genes, which revealed that *TP63*, *LURAP1L*, *HSD17B11*, *ISCU*, *PEBP1*, and *TNFAIP3* were significantly downregulated in the LUAD tissues compared to the normal tissues, while *DPP4*, *CISD2*, *IDH1*, *LONP1*, and *ELAVL1* were significantly upregulated in the LUAD tissues compared to the normal tissues (P<0.05) (*Figure 2*).

Prognostic value of the candidate genes in LUAD patients with BM

The potential impact of candidate gene expression on the clinical prognosis of patients with LUAD in TCGA database was examined. Patients with low *CISD2*, *ELAVL1*, *IDH1*, and *LONP1* expression had better OS rates (*Figure 3A*). The low expression of *CISD2*, *ELAVL1*, and *IDH1* was also associated with significantly better DSS and a significantly better PFI (P<0.05). LUAD patients with low expression of *CISD2*, *ELAVL1*, and *IDH1* have better DSS and PFI (*Figure 3B*,*3C*). Combining the expression of candidate genes in LUAD and their role in prognosis, as well as previous research reports (14,15), we selected *CISD2* as the most promising candidate gene to perform further investigations.

Determining the genes and proteins that interact with CISD2

A gene-gene interaction network of *CISD2* was established, and neighboring genes were altered via GeneMania (*Figure 4A*), and a PPI network of *CISD2* was constructed (*Figure 4B*).

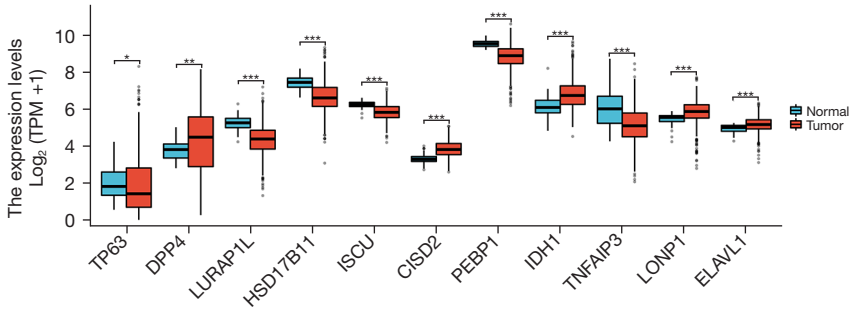

Figure 2 Expression of candidate DEGs in lung adenocarcinoma in TCGA. *, P<0.05; **, P<0.01; ***, P<0.001, statistically significant difference. DEGs, differentially expressed genes; TCGA, The Cancer Genome Atlas; TPM, transcripts per million.

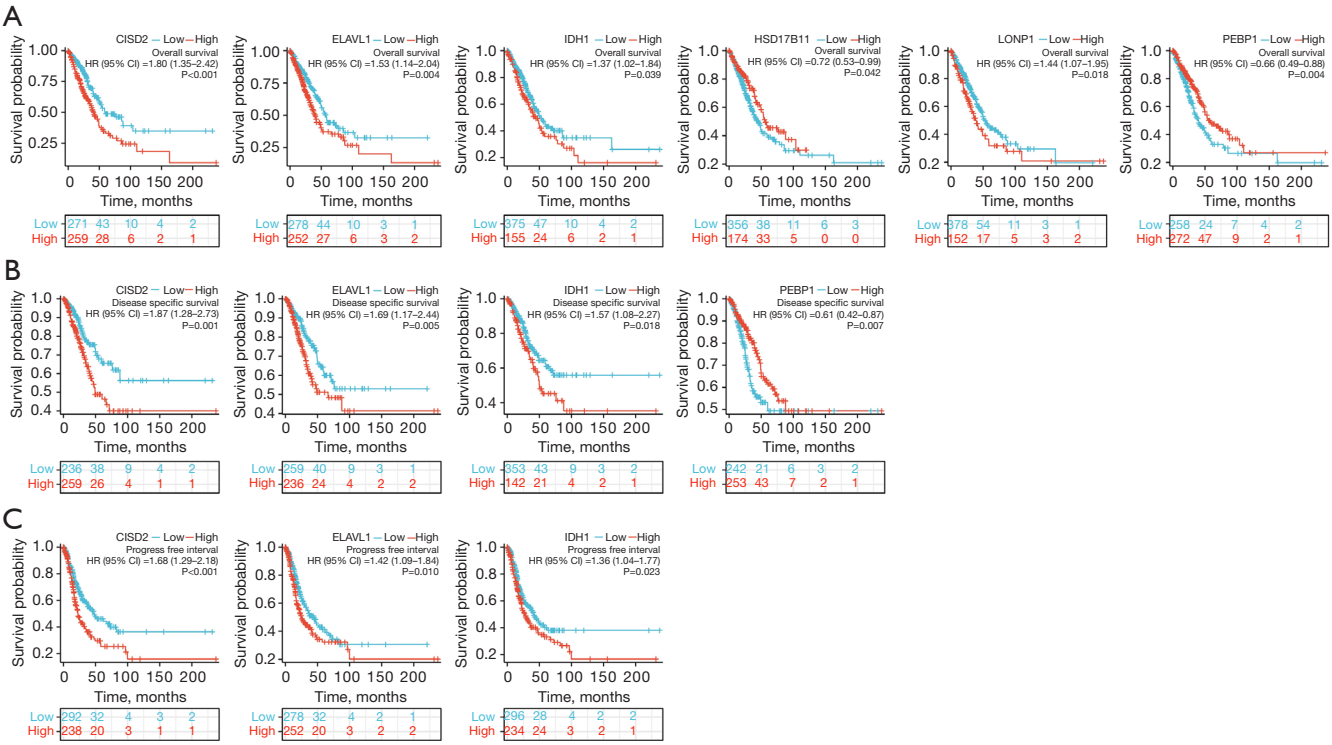

Figure 3 Correlation between candidate DEGs and the prognosis of lung adenocarcinoma patients. (A) OS; (B) DSS; and (C) PFI. DEGs, differentially expressed genes; OS, overall survival; DSS, disease-specific survival; PFI, progression-free interval.

Association between CISD2 and immune cells

The potential relationship between *CISD2* expression and the immune cell infiltration of LUAD tumors was assessed. *CISD2* levels were negatively associated with B and cluster of differentiation (CD)4 + T cell infiltration levels, but were positively associated with dendritic, CD8+ T, neutrophil, and macrophage cell infiltration levels (*Figure 5A*). To further assess the influence of *CISD2* on the tumor microenvironment (TME), the associations between *CISD2* and immune cell types were evaluated. *CISD2* levels were negatively correlated with the infiltration of most immune cells, including B cells, plasmacytoid dendritic cells, natural killer cells, and T follicular helper cells, and were positively correlated with the infiltration level of T helper cells, T helper 2 cells, and gamma delta T cells (*Figure 5B,5C*). Based on these findings, we speculate that the expression of *CISD2* may be associated with tumor immune infiltration in LUAD.

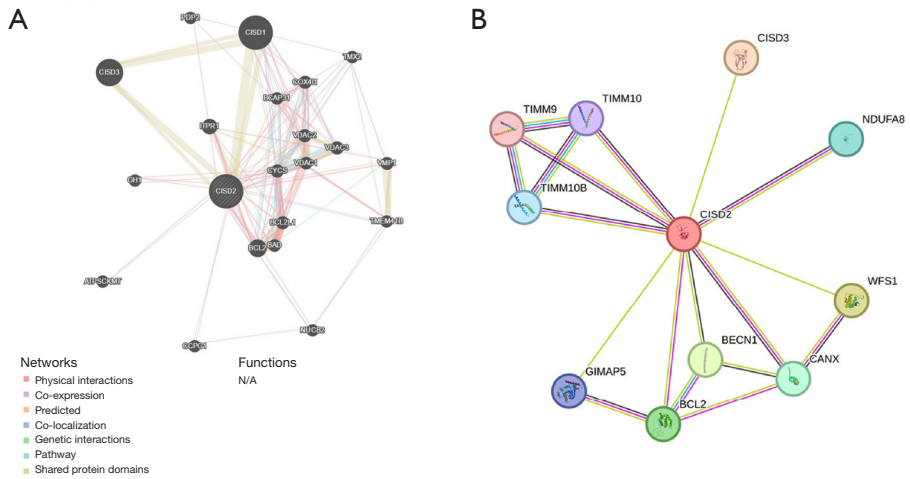

Figure 4 Screening the *CISD2*-interacting proteins and genes. (A) Gene-gene interaction network of *CISD2*; (B) PPI network of *CISD2*. PPI, protein-protein interaction.

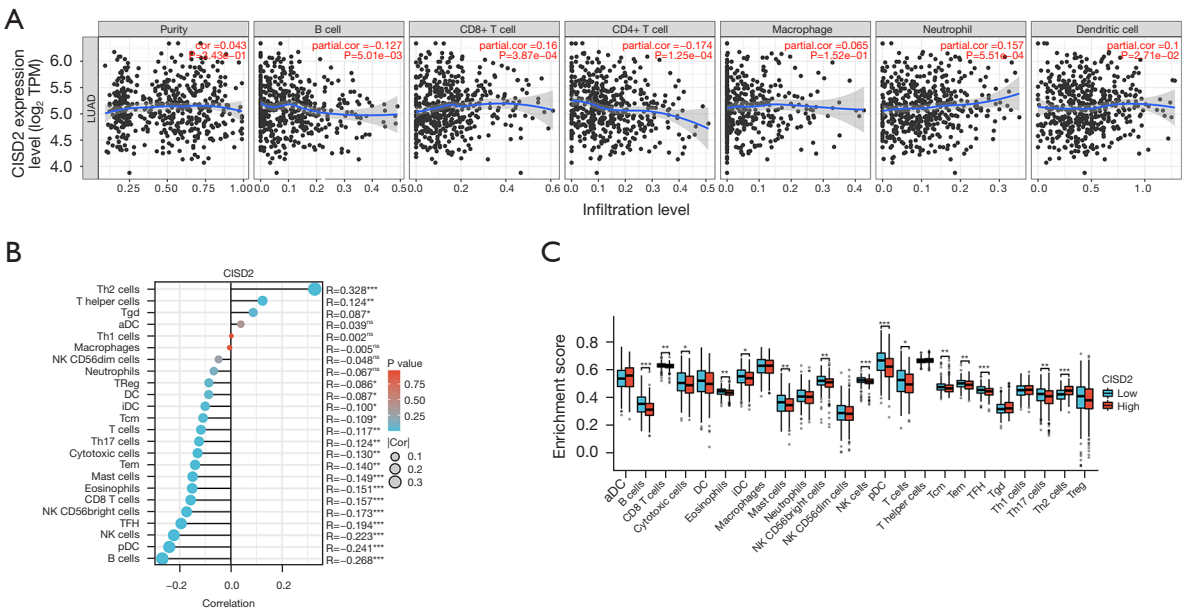

Figure 5 Correlation between *CISD2* levels and immune cell infiltration levels. (A) Correlation between *CISD2* levels and the infiltration of different immune cell types in lung adenocarcinoma in the TIMER and (B, C) TCGA database. *, P<0.05; **, P<0.01; ***, P<0.001; ns, no significant. TIMER, Tumor IMmune Estimation Resource; TCGA, The Cancer Genome Atlas.

Pathway prediction based on the GSEA

Using Metascape, an online GSEA functional analysis was carried out, which revealed that *CISD2* may affect the biological processes of LUAD by affecting the cell cycle, reactive mitochondrial translation, and DNA damage repair, and activating the *MYC* and P53 signaling pathways (*Figure 6*).

Upstream regulation of CISD2 by MiRNAs

To determine whether *CISD2* was modulated by upstream genes, the top ten predicted miRNAs that bind the 3'UTR end of *CISD2* mRNA were identified (Table S1).

In the TCGA database, exploring the expression of the above candidate miRNAs in LUAD, we found that only

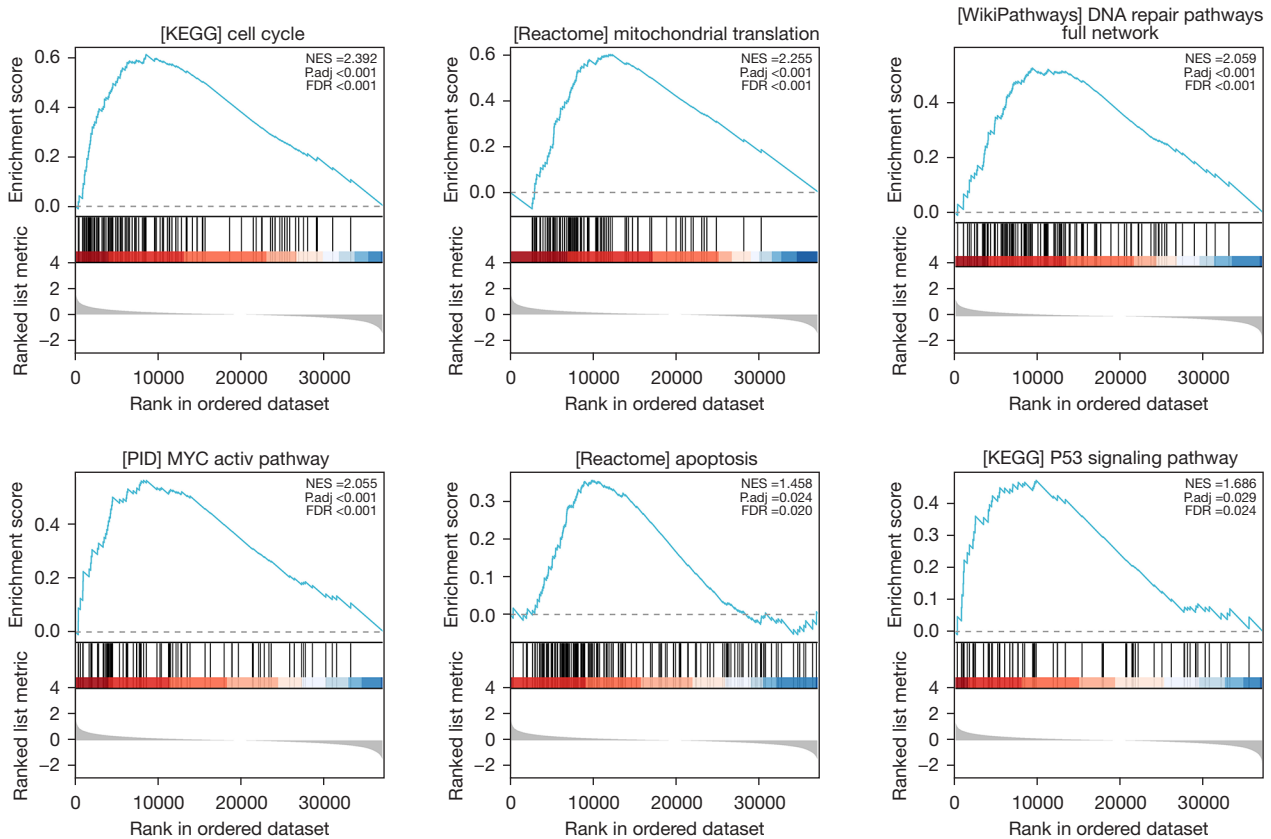

Figure 6 Possible relevant pathways from the GSEA. The Gene Ear Biology Biological Process gene set from MSigDB was used. 1,600 random sample permutations were carried out. NES, normalized enrichment score; FDR, false discovery rate; GSEA, gene set enrichment analysis.

hsa-miR-335-5p and hsa-miR-320a were downregulated in tumor tissues, while hsa-miR-186-5p, hsa-miR-199a-3p, hsa-miR-199b-3p, hsa-miR-320b, hsa-miR-320c, hsa-miR-320d, hsa-miR-154-5p, and hsa-miR-495-3p were upregulated in tumor tissues, all with statistically significant differences (P<0.05) (*Figure 7*).

We further analyzed the correlation between the above 10 candidates and *CISD2* in TCGA database. According to the competing endogenous RNA (ceRNA) hypothesis, miRNAs inhibit the expression of their target mRNAs by binding to them. Therefore, in the ceRNA network, there had to be a negative association between the miRNA and target mRNA. Combining the above-mentioned candidate miRNA expression results, correlation intensity results, and previous research reports, we ascertained that HSA-miR-320A was the most potent upstream modulator of miRNA (*Figure 8*).

Clinical outcomes

Positive expression of CISD2 in LUAD tissues

Of the 40 patients included in the study, 18 had BM, which had an incidence rate of 45.00%. The patients were divided into the BM group and non-BM group. In the BM group, CISD2 was positively expressed in 11 cases (61.11%) with an immunohistochemistry score of 3.77±2.35. In the non-BM group, CISD2 was positively expressed in six cases (27.27%) with an immunohistochemistry score of 2.29±1.68. The positive expression rate of CISD2 and the immunohistochemistry scores were significantly more increased in the BM group than the non-BM group (P<0.05) (*Figure 9* and *Table 1*).

Univariate analysis of factors influencing LUAD

The serum levels of NSE, ALP, carcinoembryonic antigen

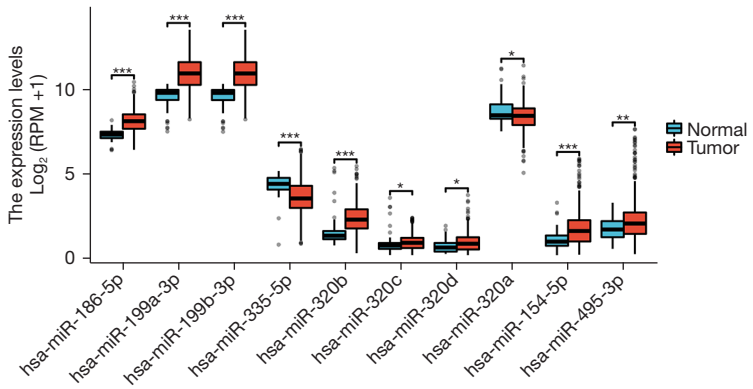

Figure 7 Expression of candidate miRNAs in LUAD in TCGA database. *, P<0.05; **, P<0.01; ***, P<0.001. TCGA, The Cancer Genome Atlas; miRNAs, microRNAs; LUAD, lung adenocarcinoma; RPM, reads per million.

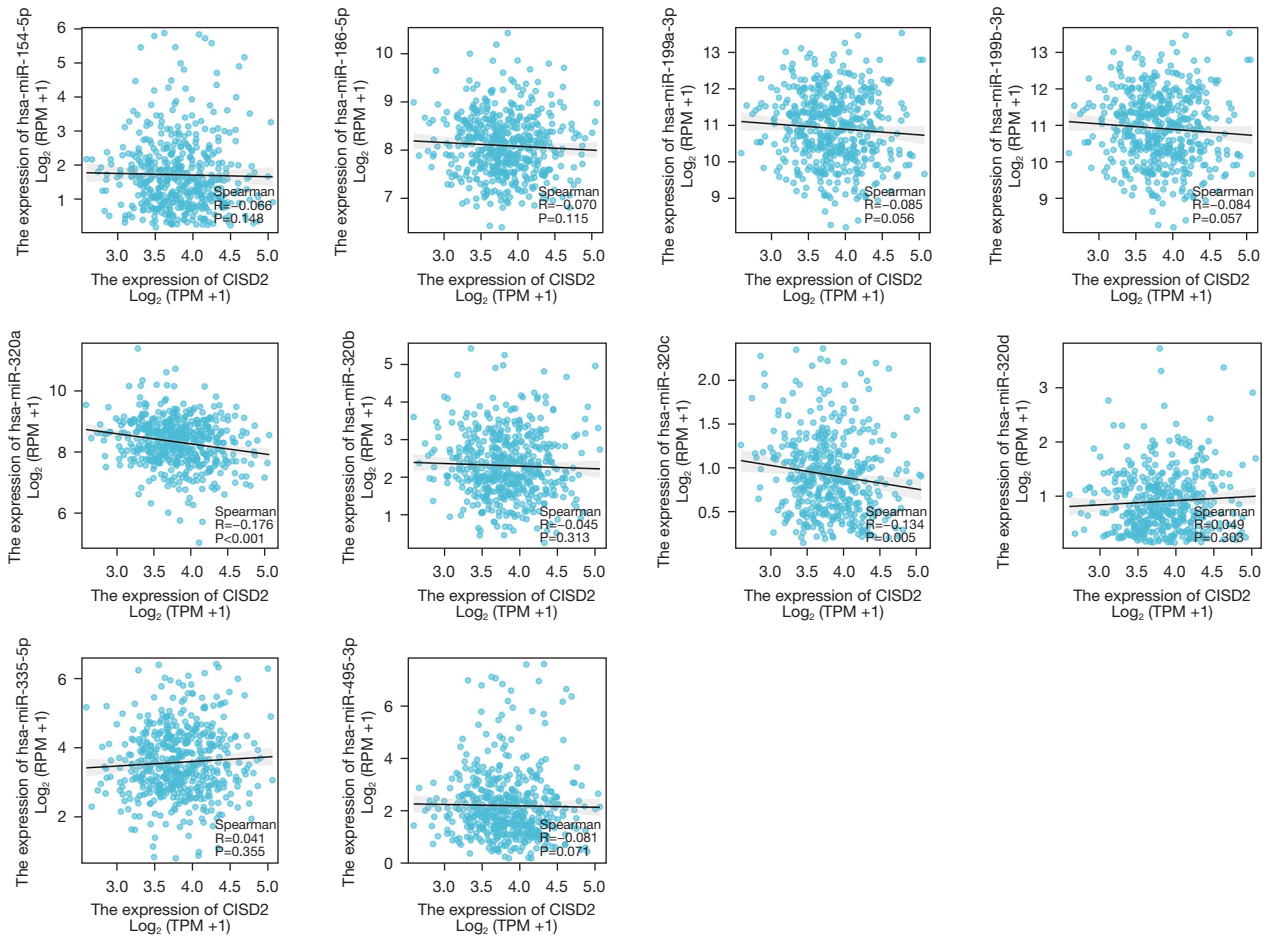

Figure 8 The association between the candidate miRNA and CISD2 in TCGA database. miRNA, microRNA; TCGA, The Cancer Genome Atlas; RPM, reads per million.

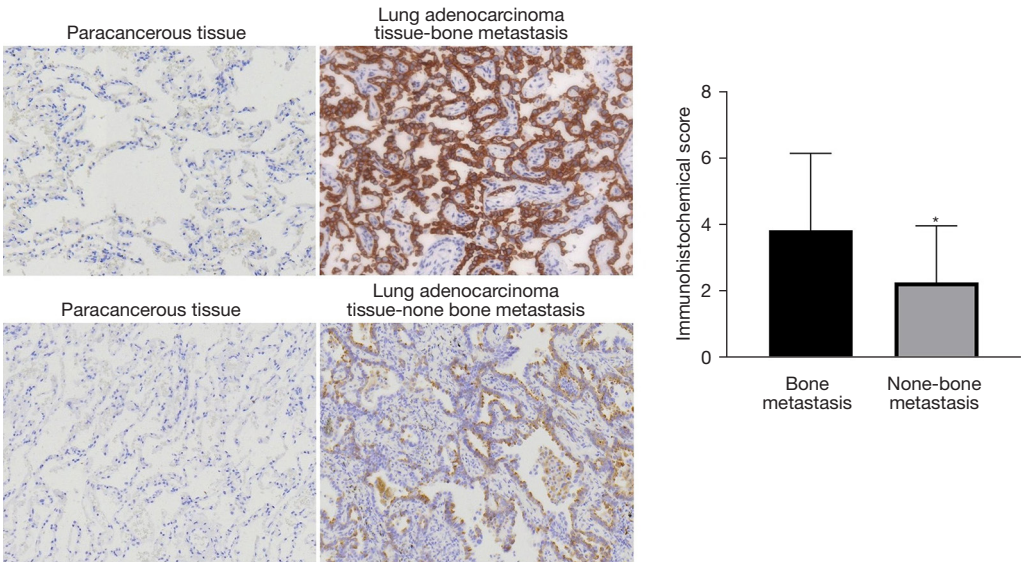

Figure 9 Immunohistochemical results of *CISD2* in lung adenocarcinoma tissues and paracancerous tissues (×200). *, P<0.05.

Table 1 Expression of CISD2 in LUAD patients with lung adenocarcinoma

CISD2 expression	BM group (n=18)	Non-BM group (n=22)	χ^2	P
Positive	11	6	4.639	0.03
Negative	7	16		

LUAD, lung adenocarcinoma; BM, bone metastasis.

(CEA), and carbohydrate antigen 125 (CA125) were higher in the BM group than the non-BM group (P<0.05). No statistically significant differences were found in terms of gender, Eastern Cooperative Oncology Group (ECOG) score, age, and smoking status (P>0.05) (see *Table 2* for more detailed data).

Binary logistic multivariate regression analysis

The factors identified as significantly different in the above univariate analysis were included in the binary logistic multivariate regression analysis. The results indicated that serum ALP and CISD2 expression are risk factors for LUAD (*Table 3*).

Discussion

In China, LC ranks first in terms of new cases and deaths, and the probability of BM is as high as 10–15%. LUAD is the most frequent pathological subtype of LC (16). Clinically, the diagnosis of LC BM mainly relies on imaging and bone puncture biopsy. Due to limitations of sensitivity, low specificity, and radiation, it is difficult to achieve early discovery and early diagnosis of BM (17). At present, the specific molecular mechanism related to the metastasis of LUAD is unclear. Therefore, in clinical practice, effective molecular tumor indices have essential reference value in the early diagnosis, prognosis evaluation, and recurrence monitoring of tumor patients.

Ferroptosis, which is a distinctive iron-dependent type of programmed cell death, is crucially involved in various pathological and physiological processes, including immunity and cancer. Relevant studies have explored its implications in tumor metastasis. For example, ferroptosis nano-therapy can simultaneously block hematogenous and lymphatic metastasis (18). *BACH1*-mediated ferroptosis modulates lymphatic metastasis by suppressing monounsaturated fatty-acid biosynthesis (19). In nasopharyngeal cancer, extracellular vesicles derived from platelets suppress ferroptosis and promote distant metastasis (20). *KLF2* regulates ferroptosis through *GPX4* to inhibit the ability of cancer cells to invade and migrate in clear cell renal cell carcinoma (21). However, currently, research on the activity of ferroptosis in LC BM is limited.

Table 2 Baseline data of LUAD patients with/without BM

Factor	BM (n=18)	No BM (n=22)	χ^2/t	P value
Sex			1.125	0.29
Male	12	11		
Female	6	11		
Age (years)	61.38±3.37	60.12±2.82	1.288	0.21
ECOG score			5.114	0.08
0	2	6		
1	8	13		
2	8	3		
ALP ($U \cdot L^{-1}$)	202.04±21.50	178.73±19.65	3.578	0.001
NSE ($\mu g \cdot L^{-1}$)	14.61±3.10	12.44±2.30	2.541	0.02
CEA (ng/mL)	7.00±1.57	6.10±1.08	2.142	0.04
CA125 (U/mL)	41.68±6.83	36.42±4.08	3.018	0.005
Smoking history			0.852	0.36
Yes	10	9		
No	8	13		

Data are presented as number or mean ± standard deviation. LUAD, lung adenocarcinoma; BM, bone metastasis; ECOG, Eastern Cooperative Oncology Group; ALP, alkaline phosphatase; CEA, carcinoembryonic antigen; CA125, carbohydrate antigen 125; NSE, neuron-specific enolase.

Table 3 Binary logistic multivariate regression analysis

Variable	Multivariate regression analysis		
	HR	95% CI	P
ALP ($U \cdot L^{-1}$)	1.061	1.007–1.119	0.03
NSE ($\mu g \cdot L^{-1}$)	1.423	0.895–2.262	0.14
CEA (ng/mL)	2.448	0.965–6.208	0.06
CA125 (U/mL)	1.133	0.928–1.384	0.22
CISD2 expression			
Positive	9.487	1.141–78.908	0.04
Negative	–	–	–

HR, hazard ratio; CI, confidence interval; ALP, alkaline phosphatase; NSE, neuron-specific enolase; CEA, carcinoembryonic antigen; CA125, carbohydrate antigen 125.

This study conducted a bioinformatics analysis to identify the ferroptosis-related DEGs in LC BM and also conducted a functional enrichment analysis. The intersection of the DEGs from the LC-BM dataset GSE10799 and ferroptosis-related genes yielded 15 candidate genes. Based on their expression in the TCGA-LUAD dataset and their impact on prognosis, three final candidate genes were identified (i.e., *CISD2*, *ELAVL1*, and *IDH1*). These genes have been investigated in the context of LUAD. For instance, in non-small-cell LC (NSCLC), the downregulation of *CISD2* has been shown to have prognostic value and to inhibit tumor development by inducing mitochondrial dysfunction (22).

Conversely, the upregulation of *CISD2* increases reactive oxygen species homeostasis, leading to tumor development and poor prognosis in LUAD (15).

ELAVL1 expression is upregulated by exosomal lncRNA FOXD3-AS1, thereby activating the PI3K/Akt pathway, which in turn increases the 5-fluorouracil resistance, invasion, and proliferation of LUAD cells (23). Considering the characteristic mechanisms of ferroptosis and previous research findings, we identified *CISD2* as the optimal select candidate gene. Through TCGA, GeneMania, and STRING databases, the protein genes that interacted with *CISD2* were identified, providing reference points for further mechanistic analyses.

In the TIMER database, the expression of *CISD2* was negatively linked with B and CD4+ T cell infiltration levels, but positively associated with macrophage, neutrophil, CD8+ T, and dendritic cell infiltration levels. While previous research has described the influence of *CISD2* on the tumor immune microenvironment in colorectal cancer and gliomas (24,25), our findings also suggest *CISD2* may affect immune infiltration in LUAD. Various types of immune cells play crucial roles in the BM of LUAD. CD8+T cells can infiltrate the BM site, directly killing metastatic cancer cells and inhibiting the progression of BM. Additionally, CD4+T cells may enhance the cytotoxic effect on BM cancer cells by promoting the activation and proliferation of CD8+T cells. These CD4+ T cells also help regulate the immune response, maintain immune system balance, and prevent excessive immune reactions that could damage the body (26). Neutrophils can secrete pro-inflammatory factors that enhance the invasive capabilities of tumor cells, promoting the survival and spread of cancer cells within bone tissue (27). Tumor-associated macrophages (TAMs) may promote angiogenesis and matrix degradation in bone metastases by secreting various growth factors and cytokines, thereby creating favorable conditions for the growth and spread of bone metastatic cancer cells. Additionally, TAMs can weaken the body's anti-tumor immune response by inhibiting the activation of immune cells (28). Additionally, the GSEA revealed that *CISD2* may impact various biological processes in LC by participating in cell-cycle regulation, reactive mitochondrial translation, DNA damage repair, *MYC* activation, and the P53 signaling pathway.

Our findings about these potential mechanisms align with previous findings on the development and progression of LC (29-32). For instance, research has shown that *CKAP2L* promotes NSCLC progression by regulating transcription elongation (29). *TRIP13* enhances LC cell growth and migration through the AKT/mTORC1/c-*MYC* signaling pathway (30). The miR-296-3p/PRKCA/FAK/Ras/c-*MYC* feedback loop modulated by the HDGF/DDX5/β-catenin complex contributes to LUAD (31). P53-induced gene 3 activates the FAK/Src pathway, promoting cell migration and invasion in LUAD (32).

Additionally, in an analysis of data from both the TargetScan and TCGA databases, hsa-miR-320a was identified as the optimal upstream regulatory miRNA of *CISD2*. hsa-miR-320a inhibits the expression of *CISD2* by directly binding to its 3'UTR region, and there is a negative correlation between the two. Research on hsa-miR-320a in LUAD supports its role as a tumor suppressor and prognostic factor (33). It is upregulated during the reversal of platinum resistance in LUAD, offering a novel approach to studying the pathogenesis of LUAD (34). MiR-320a effectively inhibits the capability of LUAD cells to proliferate and migrate by regulating the STAT3 signaling pathway (35). Combining these findings, we speculate that miR-320a, as a negative regulator of *CISD2*, may participate in LUAD BM by activating *MYC* and could be associated with tumor immune infiltration. These speculations provide valuable references for subsequent experimental investigations.

Our retrospective analysis of 40 real-world LUAD patients revealed that the positive expression rate of *CISD2* and the immunohistochemistry scores of BM patients were significantly increased compared to those of patients who did not have BM. The multivariate analysis identified serum ALP and CISD2 expression as significant risk factors for BM in LUAD patients. Elevated ALP levels have been previously associated with BM and metastatic activity (36), which supports our findings. The identification of *CISD2* as a risk factor is particularly novel, as the role of this gene in BM has not been extensively explored in LUAD. These research findings have important implications for public health and clinical practice. In public health, our study identifies *CISD2* as a potential therapeutic target for LUAD BM, providing clues for developing new anti-cancer therapies. Clinically, *CISD2* serves as a potential biomarker for patients with LUAD BM, aiding doctors in more accurately assessing patient conditions, personalizing treatment plans, and monitoring disease progression.

Conclusions

This study used biological information technology to analyze and determine the potential ferroptosis select

candidate gene *CISD2* in the pathogenesis of LUAD to provide novel targets for LUAD-BM treatment. However, this study has certain limitations, such as a small sample size, insufficient mechanism validation, and the absence of multicenter clinical trials. To address these, we plan to expand the sample size to improve statistical power, conduct further experiments to explore CISD2's role in LUAD BM and its relationship with immune infiltration and miR-320a regulation, and collaborate with multiple institutions on multicenter clinical trials to validate CISD2's predictive value and therapeutic potential in the future.

Acknowledgments

Funding: None.

Footnote

Reporting Checklist: The authors have completed the STREGA reporting checklist. Available at https://tcr.amegroups.com/article/view/10.21037/tcr-24-1188/rc

Data Sharing Statement: Available at https://tcr.amegroups.com/article/view/10.21037/tcr-24-1188/dss

Peer Review File: Available at https://tcr.amegroups.com/article/view/10.21037/tcr-24-1188/prf

Conflicts of Interest: All authors have completed the ICMJE uniform disclosure form (available at https://tcr.amegroups.com/article/view/10.21037/tcr-24-1188/coif). The authors have no conflicts of interest to declare.

Ethical Statement: The authors are accountable for all aspects of the work in ensuring that questions related to the accuracy or integrity of any part of the work are appropriately investigated and resolved. The study was conducted in accordance with the Declaration of Helsinki (as revised in 2013). The study was approved by the Ethics Committee of Quzhou People's Hospital (No. 2023-015) and informed consent was taken from all the patients.

References

1. Bray F, Laversanne M, Sung H, et al. Global cancer statistics 2022: GLOBOCAN estimates of incidence and mortality worldwide for 36 cancers in 185 countries. CA Cancer J Clin 2024;74:229-63.
2. Hirsch FR, Scagliotti GV, Mulshine JL, et al. Lung cancer: current therapies and new targeted treatments. Lancet 2017;389:299-311.
3. Siegel RL, Miller KD, Jemal A. Cancer statistics, 2018. CA Cancer J Clin 2018;68:7-30.
4. Cortez Cardoso Penha R, Smith-Byrne K, Atkins JR, et al. Common genetic variations in telomere length genes and lung cancer: a Mendelian randomisation study and its novel application in lung tumour transcriptome. Elife 2023;12:e83118.
5. Oliveira MB, Mello FC, Paschoal ME. The relationship between lung cancer histology and the clinicopathological characteristics of bone metastases. Lung Cancer 2016;96:19-24.
6. Li S, Peng Y, Weinhandl ED, et al. Estimated number of prevalent cases of metastatic bone disease in the US adult population. Clin Epidemiol 2012;4:87-93.
7. Dunne EM, Fraser IM, Liu M. Stereotactic body radiation therapy for lung, spine and oligometastatic disease: current evidence and future directions. Ann Transl Med 2018;6:283.
8. Tang J, Wang Y, Luo Y, et al. Computational advances of tumor marker selection and sample classification in cancer proteomics. Comput Struct Biotechnol J 2020;18:2012-25.
9. Wang Z, Li Y, Wang D, et al. Ferroptosis molecular inducers: A future direction for malignant tumor chemotherapy. Biocell 2022;46:1599-611.
10. Dixon SJ, Lemberg KM, Lamprecht MR, et al. Ferroptosis: an iron-dependent form of nonapoptotic cell death. Cell 2012;149:1060-72.
11. Zhang Y, Zhang Q, Wang F, et al. Activatable Semiconducting Polymer Nanoinducers Amplify Oxidative Damage via Sono-Ferroptosis for Synergistic Therapy of Bone Metastasis. Nano Lett 2023;23:7699-708.

12. Zhou Q, Xu T, Li J, et al. Identification of the potential ferroptosis key genes in lung cancer with bone metastasis. J Thorac Dis 2023;15:2708-20.
13. Zhou N, Bao J. FerrDb: a manually curated resource for regulators and markers of ferroptosis and ferroptosis-disease associations. Database (Oxford) 2020;2020:baaa021.
14. Fu Y, Chen B, Gao T, et al. CircSLC25A16 facilitates the development of non-small-cell lung cancer through the miR-335-5p/CISD2 axis. Thorac Cancer 2024;15:1490-501.
15. Li SM, Chen CH, Chen YW, et al. Upregulation of CISD2 augments ROS homeostasis and contributes to tumorigenesis and poor prognosis of lung adenocarcinoma. Sci Rep 2017;7:11893.
16. Hernandez RK, Wade SW, Reich A, et al. Incidence of bone metastases in patients with solid tumors: analysis of oncology electronic medical records in the United States. BMC Cancer 2018;18:44.
17. Youth Specialists Committee of Lung Cancer, Beijing Medical Award Foundaton, Chinese Lung Cancer Union. Expert Consensus on the Diagnosis and Treatment of Bone Metastasis in Lung Cancer (2019 Version). Zhongguo Fei Ai Za Zhi 2019;22:187-207.
18. Guo R, Deng M, Li J, et al. Depriving Tumor Cells of Ways to Metastasize: Ferroptosis Nanotherapy Blocks Both Hematogenous Metastasis and Lymphatic Metastasis. Nano Lett 2023;23:3401-11.
19. Xie X, Tian L, Zhao Y, et al. BACH1-induced ferroptosis drives lymphatic metastasis by repressing the biosynthesis of monounsaturated fatty acids. Cell Death Dis 2023;14:48.
20. Li F, Xu T, Chen P, et al. Platelet-derived extracellular vesicles inhibit ferroptosis and promote distant metastasis of nasopharyngeal carcinoma by upregulating ITGB3. Int J Biol Sci 2022;18:5858-72.
21. Lu Y, Qin H, Jiang B, et al. KLF2 inhibits cancer cell migration and invasion by regulating ferroptosis through GPX4 in clear cell renal cell carcinoma. Cancer Lett 2021;522:1-13.
22. Shao F, Li Y, Hu W, et al. Downregulation of CISD2 Has Prognostic Value in Non-Small Cell Lung Cancer and Inhibits the Tumorigenesis by Inducing Mitochondrial Dysfunction. Front Oncol 2021;10:595524.
23. Mao G, Mu Z, Wu DA. Exosomal lncRNA FOXD3-AS1 upregulates ELAVL1 expression and activates PI3K/Akt pathway to enhance lung cancer cell proliferation, invasion, and 5-fluorouracil resistance. Acta Biochim Biophys Sin (Shanghai) 2021;53:1484-94.
24. Xu Y, Tang Q, Ding N, et al. Ferroptosis-associated gene CISD2 suppresses colon cancer development by regulating tumor immune microenvironment. PeerJ 2023;11:e15476.
25. Zhang F, Cai HB, Liu HZ, et al. High Expression of CISD2 in Relation to Adverse Outcome and Abnormal Immune Cell Infiltration in Glioma. Dis Markers 2022;2022:8133505.
26. Xin Z, Qin L, Tang Y, et al. Immune mediated support of metastasis: Implication for bone invasion. Cancer Commun (Lond) 2024. [Epub ahead of print]. doi: 10.1002/cac2.12584.
27. Yan M, Zheng M, Niu R, et al. Roles of tumor-associated neutrophils in tumor metastasis and its clinical applications. Front Cell Dev Biol 2022;10:938289.
28. Tan Y, Wang M, Zhang Y, et al. Tumor-Associated Macrophages: A Potential Target for Cancer Therapy. Front Oncol 2021;11:693517.
29. Monteverde T, Sahoo S, La Montagna M, et al. CKAP2L Promotes Non-Small Cell Lung Cancer Progression through Regulation of Transcription Elongation. Cancer Res 2021;81:1719-31.
30. Cai W, Ni W, Jin Y, et al. TRIP13 promotes lung cancer cell growth and metastasis through AKT/mTORC1/c-Myc signaling. Cancer Biomark 2021;30:237-48.
31. Fu Q, Song X, Liu Z, et al. miRomics and Proteomics Reveal a miR-296-3p/PRKCA/FAK/Ras/c-Myc Feedback Loop Modulated by HDGF/DDX5/β-catenin Complex in Lung Adenocarcinoma. Clin Cancer Res 2017;23:6336-50.
32. Gu MM, Gao D, Yao PA, et al. p53-inducible gene 3 promotes cell migration and invasion by activating the FAK/Src pathway in lung adenocarcinoma. Cancer Sci 2018;109:3783-93.
33. Khandelwal A, Sharma U, Barwal TS, et al. Circulating miR-320a Acts as a Tumor Suppressor and Prognostic Factor in Non-small Cell Lung Cancer. Front Oncol 2021;11:645475.
34. Lu M, Hu C, Wu F, et al. MiR-320a is associated with cisplatin resistance in lung adenocarcinoma and its clinical value in non-small cell lung cancer: A comprehensive analysis based on microarray data. Lung Cancer 2020;147:193-7.
35. Lv Q, Hu JX, Li YJ, et al. MiR-320a effectively suppresses lung adenocarcinoma cell proliferation and

metastasis by regulating STAT3 signals. Cancer Biol Ther 2017;18:142-51.
36. Schlack K, Krabbe LM, Rahbar K, et al. ALP bouncing and LDH normalization in bone metastatic castration-resistant prostate cancer patients under therapy with Enzalutamide: an exploratory analysis. Transl Androl Urol 2021;10:3986-99.

Cite this article as: Zhao X, Li L, Li Y, Liu Y, Wang H, Tabrizi NS, Ye Z, Zhao Z. Bioinformatic prediction of miR-320a as a potential negative regulator of CDGSH iron-sulfur domain 2 (*CISD2*), involved in lung adenocarcinoma bone metastasis via MYC activation, and associated with tumor immune infiltration. Transl Cancer Res 2024;13(8):4485-4499. doi: 10.21037/tcr-24-1188

